JOURNAL OF THEORETICAL AND APPLIED MECHANICS
58, 4, pp. 971-982, Warsaw 2020
DOI: 10.15632/jtam-pl/127178

PROPAGATION OF THE TORSIONAL WAVE IN AN IRREGULAR SELF-REINFORCED COMPOSITE MATERIAL BOUNDED BETWEEN TWO HALF-SPACES

Shishir Gupta, Sandip Kumar Das
Indian Institute of Technology, Department of Mathematics and Computing, Dhanbad, Jharkhand, India
e-mail: shishir_ism@yahoo.com; skdkgpiit@gmail.com

This research article is concerned with the analytical assessment and mathematical modelling to unveil the characteristic of a torsional wave in the irregular Earth's crustal stratum. This investigation has been performed to clarify of possible occurrence of the torsional wave in an irregular self-reinforced composite layer bonded between dry sandy media and an isotropic elastic half-space. Rectangular and parabolic irregularities have been assumed at the interface of the intermediate layer and the lower half-space. In order to acquire the required dispersion equation, the appropriate boundary conditions with the assistance of displacement and stress components have been well satisfied. The effects of different affecting parameters such as reinforcement, sandiness, initial stress and irregularity parameters have been explored and explained by suitable graphs. Moreover, a comparative study has also been accomplished graphically for rectangular, parabolic, and no irregularities.

Keywards: torsional wave, phase velocity, sandy layer, irregularity, initial stress

1. Introduction

Disciplines such as seismology, solid physics, geotechnical engineering, geophysics, seismic waves have been considered extensively for salient dynamic survey equipment. The major objective of studying seismic waves is to unveil characteristic properties of different equipment inside the structure of the Earth. Some of the notable works were presented by Akbarov *et al.* (2011), Selim (2007), Ozturk and Akbarov (2009), Chattopadhyay *et al.* (2011), Gupta and Bhengra (2017a), etc.

Numerous problems associated with wave propagation in a composite medium such as fiber--reinforced medium has attracted attention of many theoretical mathematicians and geophysicists. A wide variety of applications of composite materials in the industrial area ignites the interest of many researchers towards it. Alumina, concrete, and fiberglass are examples of fiber--reinforced materials. Adkins and Rivlin (1955) established the model of continuum theory for a fiber-reinforced material later on modified by Spencer (1972) and Maugin (1981). Belfield *et al.* (1983) developed a linear model for fiber-reinforced elastic plates with the reinforcement continuously distributed in concentric circles.

The initial stress is a stress that persists in an elastic structural body, even if there are no external forces available and, therefore, the body is defined as initially stressed. In the medium, initial stresses can be triggered by both an artificial and natural mechanism. There is a possibility for the existence of initial stress inside the Earth owing to variation of temperature, pressure of atmosphere, existence of surcharge layer, creep, variation in gravity, etc. These stresses contribute a noteworthy effect on seismic wave propagation as well as the material of the medium. Biot (1940) described the vital effect of the initial stress on propagation of seismic waves. A brief discussion on the upshot of the initial stress on the torsional wave propagation was explored by

Dhua *et al.* (2015). Gupta and Bhengra (2017b) gave an extensive discussion regarding the favor of the initial stress on the soil dynamics.

The Earth's surface may not only be considered as a plane surface but a surface having irregular boundaries. Elastic wave propagation in irregular layered media has been substantially encapsulated in many research works such as Kaur and Tomar (2005), Kaur *et al.* (2005), Chattopadhyay *et al.* (2009), Singh and Sahu (2017), etc.

The present paper gives a brief mathematical overview of propagation of the torsional wave in an irregular fiber-reinforced medium bonded between an initially stressed dry sandy half-space and an isotropic elastic half-space. By utilizing dynamical equations of motion, the displacement components have been concluded separately for all three media. The dispersion equation has been acquired in a closed-form mathematically by utilizing the displacement components and suitable boundary conditions. The foremost goal of the present article is to exhibit the impact of reinforcement, sandiness, initial stress, rectangular, and parabolic irregularities and the heterogeneity parameter. To imagine the affect of these parameters, graphs have been followed independently for each parameter and displayed in detail.

2. Mathematical formulation

Let the model be subjected to a cylindrical coordinate system such that r-axis is in the direction of wave propagation and the positive z-axis is being directed along the lower half-space. The proposed model is considered with a self-reinforced composite layer clamped between a dry sandy half-space and an isotropic half-space. At the interface of the layer and the lower half--space, two types of irregularity (parabolic, rectangular) have been considered. The equations of the irregular interfaces for both cases (rectangular and parabolic) may be defined as

$$z = \varepsilon\iota(r) \tag{2.1}$$

where $\iota(r)$ and ε is mentioned in Appendix.

3. Study of the self-reinforced composite layer

The consitutive equation for a transversely isotropic linear elastic material with the preferred direction $\overrightarrow{\partial}$ is

$$\begin{aligned}\varphi_{ij} &= \lambda e_{kk}\delta_{ij} + 2\mu_T e_{ij} + \alpha_1(\partial_k\partial_m e_{km}\delta_{ij} + e_{kk}\partial_i\partial_j)\\ &\quad + 2(\mu_L - \mu_T)(\partial_i\partial_k e_{kj} + \partial_j\partial_k e_{ki}) + \beta_1\partial_k\partial_m e_{km}\partial_i\partial_j\end{aligned} \tag{3.1}$$

where $i, j, k, m = 1, 2, 3$, and φ_{ij}, e_{ij}, δ_{ij} are components of stresses, strain, and the Kronecker delta, respectively. The unit reinforcement component is defined by $\overrightarrow{\partial} = [\partial_1, \partial_2, \partial_3]$, such that $\partial_1^2 + \partial_2^2 + \partial_3^2 = 1$. μ_T, μ_L are defined as the transverse and longitudinal shear modulus, respectively.

Now, for propagation of the torsional wave, we have

$$u_r = 0 \qquad u_z = 0 \qquad u_\theta = v_1(r, z, t) \tag{3.2}$$

which gives

$$\begin{aligned}&e_{zz} = 0 \qquad e_{\theta\theta} = 0 \qquad e_{rr} = 0 \qquad e_{zr} = 0\\ &e_{r\theta} = \frac{1}{2}\Big(\frac{\partial v_1}{\partial r} - \frac{v_1}{r}\Big) \qquad e_{\theta z} = \frac{1}{2}\frac{\partial v_1}{\partial z}\end{aligned} \tag{3.3}$$

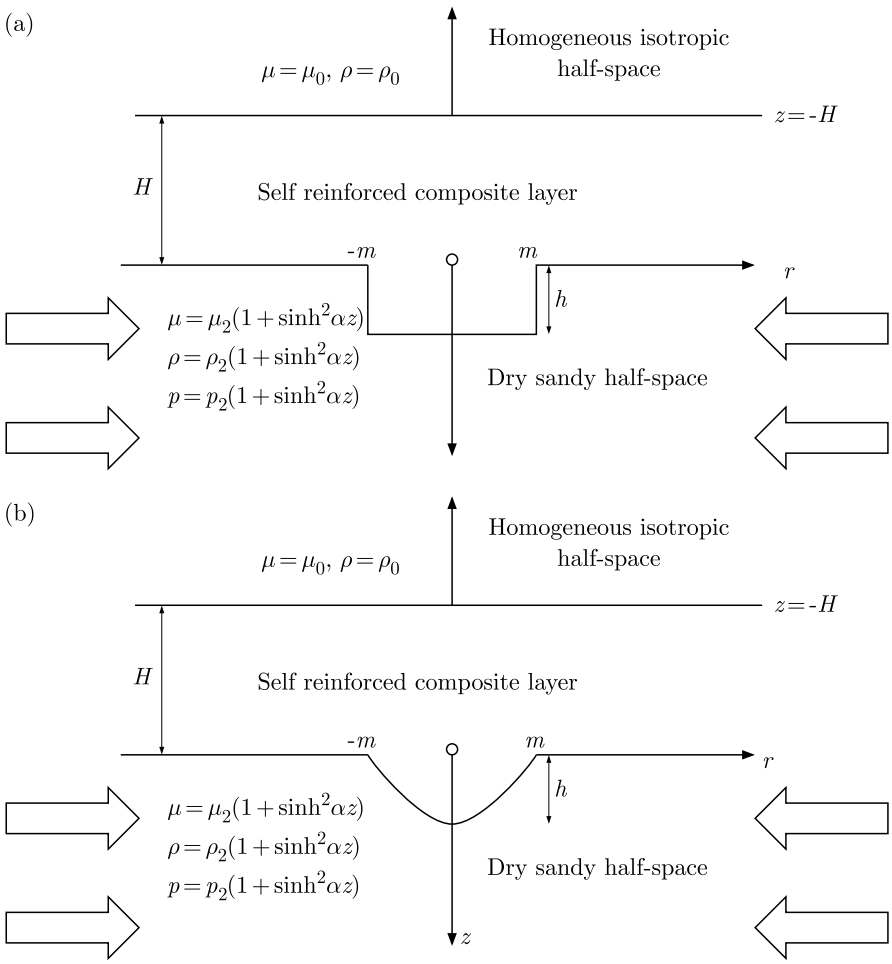

Fig. 1. Geometrical formulation of the proposed model: (a) with rectangular irregularity, (b) with parabolic irregularity

Using Eqs. (3.2) and (3.3) in Eq. (3.1), the non vanishing stress components are as follows

$$\varphi_{\theta z}=R\frac{\partial v}{\partial r}-\frac{v_1}{r}\qquad \varphi_{r\theta}=S\Big(\frac{\partial v_1}{\partial r}-\frac{v_1}{r}\Big)+Q\frac{\partial v_1}{\partial z} \tag{3.4}$$

where

$$R=\mu_T+\partial_3^2(\mu_L-\mu_T)\qquad S=\mu_T+\partial_1^2(\mu_L-\mu_T)\qquad Q=\partial_1\partial_3(\mu_L-\mu_T) \tag{3.5}$$

Applying the above

$$\frac{\partial\varphi_{r\theta}}{\partial r}+\frac{\partial\varphi_{\theta z}}{\partial z}+\frac{2}{r}\varphi_{r\theta}=\rho_1\frac{\partial v_1}{\partial t} \tag{3.6}$$

where ρ_1 is density of the intermediate layer.

In view of Eqs. (3.4) and (3.6) one obtains

$$R\frac{\partial^2 v_1}{\partial z^2}+2Q\frac{\partial^2 v_1}{\partial r\partial z}+S\frac{\partial^2 v_1}{\partial r^2}+\frac{Q}{r}\frac{\partial v_1}{\partial z}+\frac{S}{r}\Big(\frac{\partial v_1}{\partial r}-\frac{v_1}{r}\Big)=\rho_1\frac{\partial^2 v_1}{\partial t^2} \tag{3.7}$$

The solution to Eq. (3.7) may be taken as

$$v_1=V_1(z)J_1(kr)\mathrm{e}^{\mathrm{i}\omega t} \tag{3.8}$$

where $J_1(kr)$ and ω are mentioned in Appendix.

Equation (3.7) with the help of Eq. (3.8) becomes

$$\frac{d^2V_1}{dz^2} + L\frac{dV_1}{dz} + MV_1 = 0 \tag{3.9}$$

where L, M are defined in Appendix.

From Eq. (3.9), we have

$$V_1 = \mathrm{e}^{-\frac{Lz}{2}}(A_2 \sin\sqrt{N}z + A_3 \cos\sqrt{N}z) \tag{3.10}$$

where $N = M - L^2/4$, and L, M, N, A_2, A_3 are all constants.

Hence, the displacement of the self-reinforced medium is given by

$$v_1 = \mathrm{e}^{-\frac{Lz}{2}}(A_2 \sin\sqrt{N}z + A_3 \cos\sqrt{N}z)J_1(kr)\mathrm{e}^{\mathrm{i}\omega t} \tag{3.11}$$

4. Study of the upper half space

The equations of motion without body forces in cylindrical coordinates are given by

$$\begin{aligned}
&\frac{\partial\varphi_{rr}}{\partial r} + \frac{1}{r}\frac{\varphi_{r\theta}}{\partial\theta} + \frac{\partial\varphi_{rz}}{\partial z} + \frac{\varphi_{rr} - \varphi_{\theta\theta}}{r} = \rho\frac{\partial^2 u_0}{\partial t^2}\\
&\frac{\partial\varphi_{r\theta}}{\partial r} + \frac{1}{r}\frac{\varphi_{\theta\theta}}{\partial\theta} + \frac{\partial\varphi_{\theta z}}{\partial z} + \frac{2}{r}\varphi_{r\theta} = \rho\frac{\partial^2 v_0}{\partial t^2}\\
&\frac{\partial\varphi_{rz}}{\partial r} + \frac{1}{r}\frac{\varphi_{\theta z}}{\partial\theta} + \frac{\partial\varphi_{zz}}{\partial z} + \frac{1}{r}\varphi_{rz} = \rho\frac{\partial^2 w_0}{\partial t^2}
\end{aligned} \tag{4.1}$$

where φ_{rr}, $\varphi_{\theta\theta}$, φ_{zz}, φ_{rz}, $\varphi_{r\theta}$ and $\varphi_{\theta z}$ are stress components. u_0, v_0 and w_0 are displacement components. Now the relation between stress and strain are given by

$$\varphi_{ij} = \lambda\Omega\delta_{ij} + 2\mu e_{ij} \tag{4.2}$$

where μ ,λ are Lame's constants, $e_{ii} = \Omega$, and e_{ij} is mentioned in Appendix.

For torsional wave propagation

$$u_0 = 0 \qquad w_0 = 0 \qquad v_0 = v_0(r, z, t) \tag{4.3}$$

Using the above equations, we have

$$\frac{\partial\varphi_{r\theta}}{\partial r} + \frac{\partial\varphi_{\theta z}}{\partial z} + \frac{2}{r}\varphi_{r\theta} = \rho\frac{\partial^2 v_0}{\partial t^2} \tag{4.4}$$

where

$$\varphi_{r\theta} = \mu\Big(\frac{\partial v_0}{\partial r} - \frac{v_0}{r}\Big) \qquad \varphi_{z\theta} = \mu\frac{\partial v_0}{\partial z} \tag{4.5}$$

Using Eq. (4.5), Eq. (4.4) reduces to

$$\mu(z)\Big(\frac{\partial^2}{\partial r^2} + \frac{1}{r}\frac{\partial}{\partial r} - \frac{1}{r^2}\Big)v_0 + \frac{\partial}{\partial z}\Big(\mu(z)\frac{\partial v_0}{\partial z}\Big) = \rho(z)\frac{\partial^2 v_0}{\partial t^2} \tag{4.6}$$

Consider the solution

$$v_0 = V_0(z)J_1(kr)\mathrm{e}^{\mathrm{i}\omega t} \tag{4.7}$$

where $J_1(kr)$ and ω are defined in Appendix.

Using Eq. (4.7) in (4.6), we have

$$\frac{d^2V_0}{dz^2} + \frac{\mu'(z)}{\mu(z)}\frac{dV_0}{dz} - k^2\Big(1 - \frac{c^2}{c_s^2}\Big)V_0(z) = 0 \tag{4.8}$$

where $c = \omega/k$, $c_s = \sqrt{\mu/\rho}$.

Rigidity and density of the uppermost half-space are

$$\mu = \mu_0 \qquad \text{and} \qquad \rho = \rho_0 \tag{4.9}$$

Using Eq. (4.9), Eq. (4.8) reduces to

$$\frac{d^2V_0}{dz^2} - m_0^2V_0(z) = 0 \tag{4.10}$$

where m_0 and shear velocity c_0 are mentioned in Appendix.

The suitable solution to Eq. (4.10) is

$$V_0 = A_1\mathrm{e}^{m_0z} \tag{4.11}$$

where A_1 is an arbitrary constant. Hence, the displacement component in the homogeneous upper half space is

$$v_0 = A_1\mathrm{e}^{m_0z}J_1(kr)\mathrm{e}^{\mathrm{i}\omega t} \tag{4.12}$$

5. Study of the lower half space

The equation of motion for the initially stressed dry sandy mantle is given by

$$\frac{\partial\Psi_{r\theta}}{\partial r} + \frac{\partial\Psi_{z\theta}}{\partial z} + \frac{2}{r}\Psi_{r\theta} + \frac{\partial}{\partial z}(Pe_{z\theta}) = \rho\frac{\partial^2v_2}{\partial t^2} \tag{5.1}$$

where $v_2 = v_2(r, z, t)$, $N = \eta\mu$, where η is the sandy parameter.

Rigidity, initial stress, density of the lowermost half-space are assumed as

$$\mu = \mu_2[1 + \sinh^2(\alpha z)] \qquad P = P_2[1 + \sinh^2(\alpha z)] \qquad \rho = \rho_2[1 + \sinh^2(\alpha z)] \tag{5.2}$$

where

$$\Psi_{r\theta} = 2Ne_{r\theta} \qquad \Psi_{z\theta} = 2Le_{r\theta} \qquad e_{r\theta} = \frac{1}{2}\Big(\frac{\partial v}{\partial r} - \frac{v}{r}\Big) \qquad e_{r\theta} = \frac{1}{2}\frac{\partial v}{\partial z}$$

Using the above relations in Eq. (5.1), we have

$$N\Big(\frac{\partial^2v_2}{\partial r^2} + \frac{1}{r}\frac{\partial v_2}{\partial r} - \frac{v_2}{r^2}\Big) + \frac{\partial}{\partial z}\Big(\delta\frac{\partial v_2}{\partial z}\Big) = \rho\frac{\partial^2v_2}{\partial t^2} \tag{5.3}$$

where $\delta = N + p/2$.

The solution to Eq. (5.3) is taken as

$$v_2 = V_2(z)J_1(kr)\mathrm{e}^{\mathrm{i}\omega t} \tag{5.4}$$

where $J_1(kr)$ and ω are mentioned in Appendix. So, Eq. (5.3) reduces to

$$\frac{d^2V_2(z)}{dz^2} + \frac{1}{\delta}\frac{dV_2(z)}{dz}\frac{d\delta}{dz} - \frac{k^2N}{\delta}\Big(1 - \frac{\rho c^2}{N}\Big)V_2(z) = 0 \tag{5.5}$$

Now substituting $V_2(z) = V_\theta(z)/\sqrt{\delta}$ in Eq. (5.5), we have

$$\frac{d^2 v_\theta(z)}{dz^2} - \frac{1}{2\delta}\Big[\frac{d^2\delta}{dz^2} - \Big(\frac{d\delta}{dz}\Big)^2\Big] v_\theta(z) = \frac{K^2 N}{\delta}\Big(1 - \frac{\rho c^2}{N}\Big) v_\theta(z) \tag{5.6}$$

Using hyperbolic variation in Eq. (5.6), then Eq. (5.6) reduces to

$$\frac{d^2 v_\theta(z)}{dz^2} - \beta^2 v_\theta(z) = 0 \tag{5.7}$$

where the values of β, ξ_2 and c_2 are given in the Appendix.

The solution to Eq. (5.7) is obtained by $v_\theta(z) = A_4 \exp(-\beta z) + A_5 \exp(\beta z)$.

The solution to Eq. (5.7), satisfying the boundary condition $v_3(z) \to 0$ as $z \to \infty$, is given by $v_\theta(z) = A_4 \exp(\beta z)$.

Thus, the displacement in the dry sandy lower half space is

$$v_2(z) = \frac{A_4 \mathrm{e}^{-\beta z}}{\sqrt{\Big(\eta\mu_2 + \frac{p_2}{2}\Big)[1 + \sinh^2(\alpha z)]}} J_1(kr)\mathrm{e}^{\mathrm{i}\omega t} \tag{5.8}$$

where $\delta = (\eta\mu_2 + p_2/2)[1 + \sinh^2(\alpha z)]$.

6. Boundary conditions of the problem

(1) Continuity of displacement holds at the interface of the uppermost half-space and the intermediate layer, i.e.

$$\begin{aligned} &(i) \quad v_1(z) = v_2(z) \qquad \text{at} \quad z = -H \\ &(ii) \quad \mu_0 \frac{\partial v_0}{\partial z} = R\frac{\partial v_1}{\partial z} + Q\Big(\frac{\partial v_1}{\partial r} - \frac{v_1}{r}\Big) \qquad \text{at} \quad z = -H \end{aligned} \tag{6.1}$$

(2) Displacement and stresses are continuous at the irregular interface of the lowermost half--space and the intermediate layer, i.e.

$$\begin{aligned} &(i) \quad v_1(z) = v_2(z) \qquad \text{at} \quad z = \varepsilon\iota(r) \\ &(ii) \quad \varphi_{\theta z} - \varepsilon\iota'(r)\varphi_{r\theta} = \Psi_{\theta z} - \varepsilon\iota'(r)\Psi_{r\theta} \qquad \text{at} \quad z = \varepsilon\iota(r) \end{aligned} \tag{6.2}$$

Using Eqs. (3.11), (4.12) and (5.8) in the above four equations, the following equations are derived

$$\begin{aligned} &A_1 \mathrm{e}^{-moH} + A_2 \mathrm{e}^{\frac{LH}{2}} \sin(\sqrt{N}H) - A_3 \mathrm{e}^{\frac{LH}{2}} \cos(\sqrt{N}H) = 0 \\ &A_1\mu_0 m_0 \mathrm{e}^{-m_0 H} - A_2 \mathrm{e}^{\frac{LH}{2}} \Big(\frac{RL}{2}\sin(\sqrt{N}H) + R\sqrt{N}cos(\sqrt{N}H)\Big) - QJ(kr)\sin(\sqrt{N}H)\Big) \\ &\quad - A_3 \mathrm{e}^{\frac{LH}{2}} \Big(-\frac{RL}{2}\cos(\sqrt{N}H) + R\sqrt{N}\sin(\sqrt{N}H) + QJ(kr)\cos(\sqrt{N}H) = 0 \\ &A_2 \mathrm{e}^{-}\frac{L\varepsilon\iota(r)}{2}\sin\left(\sqrt{N}\varepsilon\iota(r)\right) + A_3 \mathrm{e}^{-}\frac{L\varepsilon\iota(r)}{2}\cos\left(\sqrt{N}\varepsilon\iota(r)\right) - \frac{A_4}{T}\mathrm{e}^{-}(\beta\varepsilon\iota(r)) = 0 \\ &A_2 \mathrm{e}^{-}\frac{L\varepsilon\iota(r)}{2}\Big[A\sqrt{N}cos\left(\sqrt{N}\varepsilon\iota(r)\right) - \frac{AL}{2}sin\left(\sqrt{N}\varepsilon\iota(r)\right) + BJ(kr)\sin\left(\sqrt{N}\varepsilon\iota(r)\right)\Big] \\ &\quad + A_3 \mathrm{e}^{-}\frac{L\varepsilon\iota(r)}{2}\Big[-A\sqrt{N}\sin\left(\sqrt{N}\varepsilon\iota(r)\right) - \frac{AL}{2}\cos\left(\sqrt{N}\varepsilon\iota(r)\right) + BJ(kr)\cos\left(\sqrt{N}\varepsilon\iota(r)\right)\Big] \\ &\quad - A_4\eta\mu_2 \mathrm{e}^{-}\beta\varepsilon\iota(r)Y = 0 \end{aligned} \tag{6.3}$$

Solving Eqs. (6.3), we finally obtain

$$\tan\left(\sqrt{N}H+\sqrt{N}\varepsilon\iota(r)\right) = \frac{AQ\sqrt{N}J(kr)+BR\sqrt{N}J(kr)-\eta\mu_2 YTR\sqrt{N}-\mu_0 m_0 A\sqrt{N}}{BQJ^2(kr)-\frac{ALQ}{2}J(kr)-\frac{BRL}{2}J(kr)+\frac{ARL^2}{4}+ARN-\mu_2 TY\left(QJ(kr)-\frac{RL}{2}\right)\Big)} \tag{6.4}$$

where A, B, $J(kr)$, Y, N, Q, L are mentioned in Appendix.

Equation (6.4) is the required dispersion equation of the torsional wave in the irregular self-reinforced composite layer bonded between dry the sandy media and the isotropic elastic half-space.

7. Particular case

Case 1

If we take $\mu_L=\mu_T=\mu_1(say)$, then Eq. (6.4) assumes the form

$$\begin{aligned}\tan\left(kH+k\varepsilon\iota(r)\sqrt{\frac{c^2}{c_1^2}-1}\right) &= \frac{1}{\mu_1^2 k\sqrt{\frac{c^2}{c_1^2}-1}}\\ &\cdot\left\{\frac{2\mu_1^2\varepsilon\iota'(r)}{r}+\eta\mu_1\mu_2\Big[\beta+\frac{\sinh\left(2\alpha\varepsilon\iota(r)\right)}{1+\sinh^2\left(\varepsilon\iota(r)\right)}+\varepsilon\iota'(r)J(kr)\Big]+m_0\mu_0\mu_1\right\}\end{aligned} \tag{7.1}$$

This is the dispersion equation of the torsional wave in the irregular isotropic layer bounded between the isotropic half-space and the initially stressed dry sandy stratum.

Case 2

If we consider $\varepsilon=0$, $P=0$ in (7.1), then it takes the form

$$\tan\left(kH\sqrt{\frac{c^2}{c_1^2}-1}\right)=\frac{\eta\mu_1\mu_2\sqrt{\left(1-\frac{c^2}{\eta c_2^2}\right)}+\mu_0\mu_1\sqrt{1-\frac{c^2}{c_0^2}}}{\mu_1^2\sqrt{\frac{c^2}{c_1^2}-1}} \tag{7.2}$$

This is the dispersion equation of the torsional wave in the isotropic layer bounded between the isotropic half-space and the isotopic dry sandy mantle.

Case 3

Again, if we eliminate the lower half-space, dispersion Eq. (7.2) takes the form

$$\tan\left(kH\sqrt{\frac{c^2}{c_1^2}-1}\right)=\frac{\mu_0\sqrt{1-\frac{c^2}{c_0^2}}}{\mu_1\sqrt{\frac{c^2}{c_1^2}-1}} \tag{7.3}$$

This is the classical Love wave equation which validates the problem.

8. Numerical results and discussion

For the self-reinforced composite layer (Markham, 1970): $\mu_L = 56.6 \cdot 10^8\,\mathrm{N/m^2}$, $\mu_T = 24.6 \cdot 10^8\,\mathrm{N/m^2}$, $\alpha_1 = -1.28 \cdot 10^9\,\mathrm{N/m^2}$, $\beta_1 = 2209.0 \cdot 10^8\,\mathrm{N/m^2}$, $\lambda = 5.65 \cdot 10^8$, $\rho = 7800\,\mathrm{Kg/m^3}$.

For the homogeneous isotropic half-space and for the sandy half-space, the data have been taken from Gubbins (1990) as $\mu_0 = 323 \cdot 10^8\,\mathrm{N/m^2}$, $\rho_0 = 2802\,\mathrm{Kg/m^3}$, $\mu_2 = 65.4 \cdot 10^9\,\mathrm{N/m^2}$, $\rho_2 = 3409\,\mathrm{Kg/m^3}$. Moreover, the following data has been used: $a_1 = 0.00316227$, $a_3 = 0.999995$, $kr = 5$.

Figure 2a displays that for the increasing value of α/k, the phase speed increases. From this figure, it can be seen that the curves are getting accumulated at the higher frequency region. So the impact of this parameter is too low at that region. Figure 2b manifests the upshot of the sandiness η present in the lowermost half-space. This figure ensures that phase velocity is growing proportionally to the increasing value of this parameter. Figure 2c was drawn for a better understanding of the effect of the initial stress $P > 0$. We observed that the increasing value of initial stress decreased the phase velocity. Figure 2d shows the scattering curves for the torsional wave when the tensile initial stress $P < 0$ has been taken under consideration. From this figure, we observe that the phase velocity is growing proportionally with the tensile initial stress.

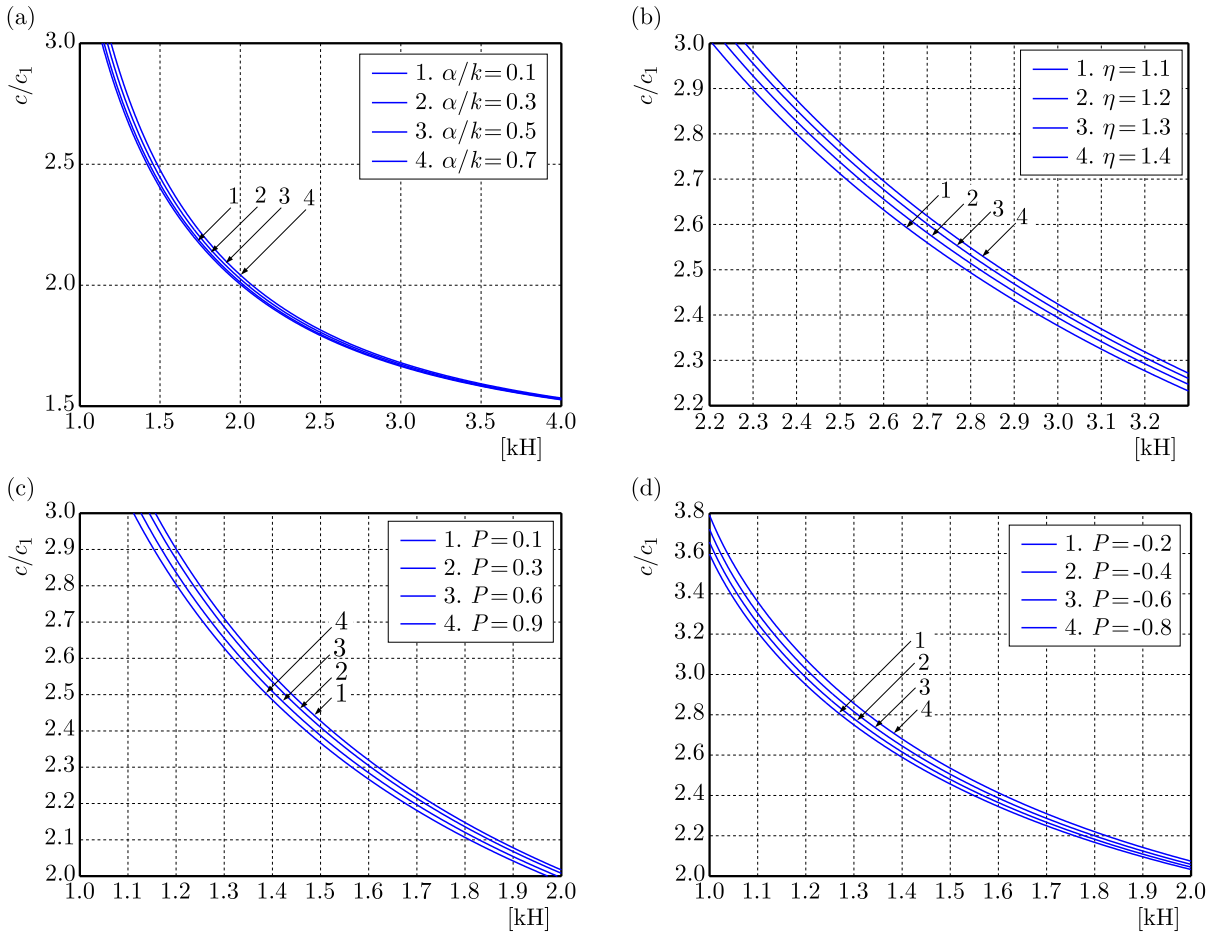

Fig. 2. Fluctuation of the phase velocity with reference to the wave number: (a) for different values of the inhomogeneity parameter $1/bk$, (b) for different values of the sandy parameter η, (c) for different values of the initial stress acting on the half-space, (d) for different values of the tensile initial stress acting on the half-space

Figure 3a displays a noteworthy result of the phase speed of the torsional wave versus the dimensionless wave number kH for distinct values of h/H. It is observed that as h/H increases, the phase speed diminishes. In Fig. 3b, a study has been carried out to get the impact of μ_L/μ_T. It is seen that the increasing value of μ_L/μ_T diminishes the phase velocity. Figure 3c expresses the impact of reinforced parameters on the torsional wave propagation. The scattering curves have been traced for distinct values of reinforcement a_1^2, a_3^2. From the figure, it has been found that as a_1 increases, as well as a_3 diminishes, the velocity of torsional wave diminishes. Hence, the torsional wave speed emphatically depends on the reinforced parameters. Figure 3d shows the refinement of phase speed of the torsional wave aligned with the dimensionless wave number kH for different sizes of the irregular parameter ε. From this figure, it is seen that the irregularity parameter encompasses a recognizable impact on the torsional wave propagation. A rising value of ε reduces the phase speed at a specific frequency.

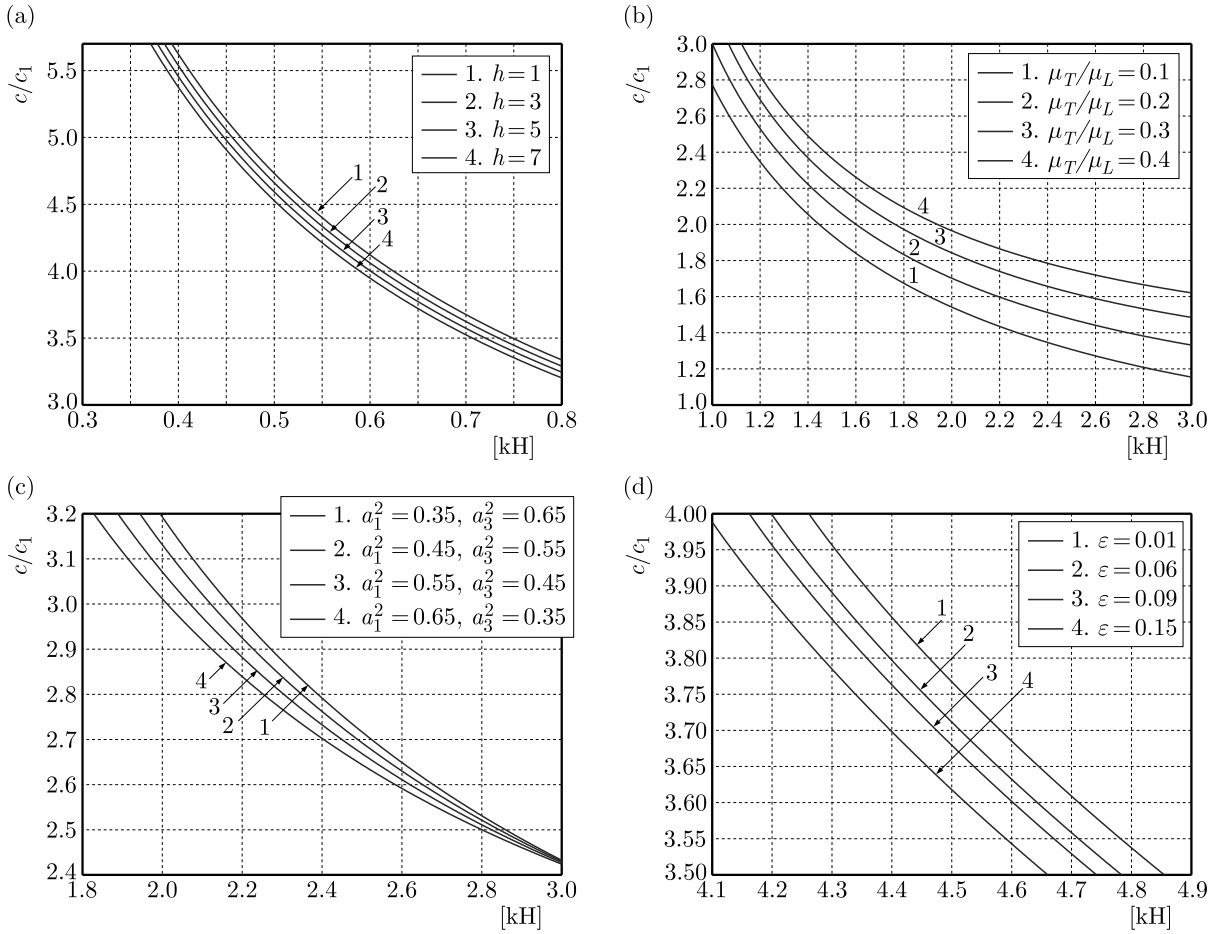

Fig. 3. Fluctuation of the phase velocity with reference to the wave number: (a) for different values of h/H, (b) for different values of μ_T/μ_L, (c) for different values of the reinforcement parameter, (d) for different values of the irregularity parameter ϵ

Figure 4a demonstrates variation of the phase velocity versus the dimensionless wave number kH for different kinds of irregularity, specifically rectangular, parabolic and no irregularity. From this figure, one can see that the phase velocity is more impacted by the presence of rectangular irregularity, which means that the phase velocity is getting smaller in the presence of rectangular irregularity. Figure 4b presents a comparative study of the phase velocity of the torsional wave with and without the self-reinforced parameter under the effect of different kinds of irregularity. Clearly from this figure, it is observed that the phase velocity is less in the presence of reinforcement.

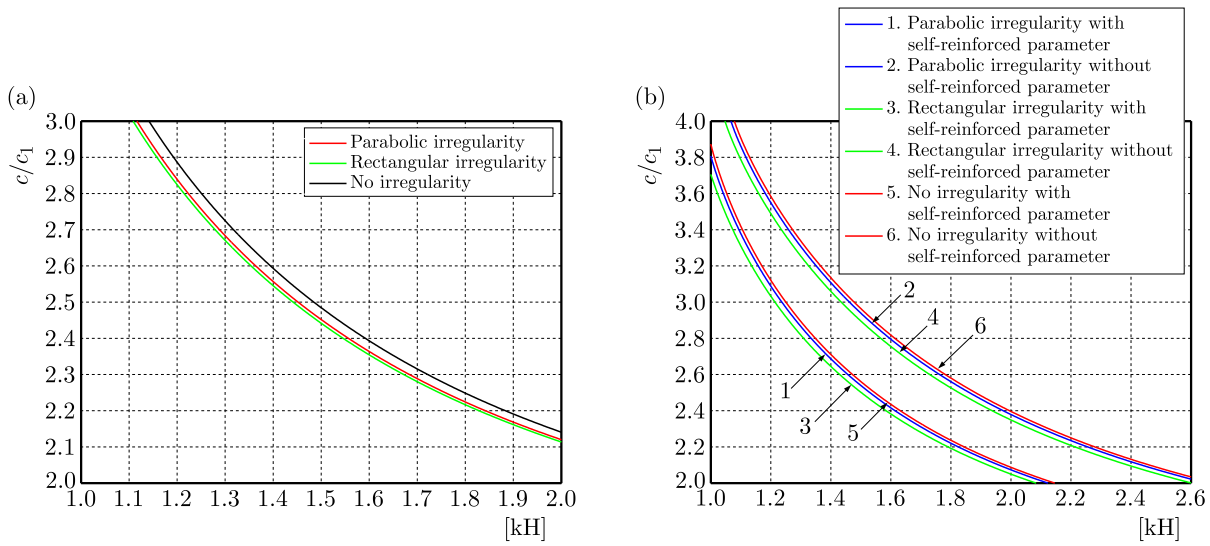

Fig. 4. Fluctuation of the phase velocity with reference to the wave number: (a) for different kinds of irregularity, (b) for different kinds of irregularity in the presence and absence of the reinforcement parameter

9. Conclusions

The prime intention of the current work is to elaborate the impact of reinforcement, sandiness, inhomogeneity, initial stress and irregularity on the torsional wave propagation. The dispersion equation has been evaluated in a closed form for the considered model. With the assistance of the dispersion equation, the impact of all the influencing parameters on the phase velocity has been well exhibited graphically. Some salient points are given below:

(i) A magnitude increment of the wave number enlarges the phase velocity, i.e. the increasing magnitude of the wave velocity increases the phase velocity.
(ii) A rising value of the inhomogeneity parameter amplifies the phase velocity.
(iii) A raising value of the sandiness parameter connected with the lower half-space possesses a favourable impact on the phase velocity.
(iv) The phase velocity decreases with the increasing amplitude of compressive initial stress, whereas the phase velocity increases with a decrease in the amplitude of tensile initial stress.
(v) Increasing values of the dimensionless parameter h/H, ε and the reinforcement diminishes the phase velocity.

A substantial review of the present paper may contribute to the analysis of problems of seismic wave propagation, signal and vibrations while studying seismic data, geophysical observations of the layered structure having dissimilar characteristic properties and containing irregularities caused by mountain roots, continental margin, etc. These outcomes can also be employed as the foundational sequence for examination of underground formations.

Appendix

i. In the case of rectangular irregularity, the function $\iota(r)$ can be defined as

$$\iota(r) = \begin{cases} h & \text{for} \quad |r| \leqslant m \\ 0 & \text{for} \quad |r| > m \end{cases}$$

In the case of parabolic irregularity, the function $\iota(r)$ can be defined as

$$\iota(r) = \begin{cases} h\Big(1 - \dfrac{r^2}{m^2}\Big) & \text{for} \quad |r| \leqslant m \\ 0 & \text{for} \quad |r| > m \end{cases}$$

where

$$\varepsilon = \frac{h}{2m} \qquad \varepsilon \ll 1$$

ii. The strain components are characterized as

$$e_{ij} = \frac{1}{2}(u_{ij} + u_{ji}) \qquad i, j = 1, 2, 3$$

iii. $J_1(kr)$ is the 1st kind Bessel function of the order one.

iv. $c_0 = \sqrt{\dfrac{\mu_0}{\rho_0}}$, $c_2 = \sqrt{\dfrac{\mu_2}{\rho_2}}$

v. $m_0 = k\sqrt{1 - \dfrac{c^2}{c_0^2}}$

vi. $\beta = k\sqrt{\dfrac{\alpha^2}{k^2} + \dfrac{1 - \frac{c^2}{\eta c_2^2}}{1 + \xi_2}}$ where $\xi_2 = \dfrac{P_2}{2\eta\mu_2}$

vii. $L = \dfrac{2QkJ_1'(kr)}{RJ_1(kr)} + \dfrac{Q}{Rr}$ and

$$M = \frac{Sk^2J_1''(kr)}{RJ_1(kr)} + \frac{SKJ_1'(kr)}{RrJ_1(kr)} + \frac{\rho\omega^2}{R} - \frac{S}{Rr^2}$$

viii. $A = R - \varepsilon\iota'(r)Q$, $B = Q - \varepsilon\iota'(r)S$ and

$$T = \sqrt{(\eta\mu_2 + \frac{P_2}{2})[1 + \sinh^2(\alpha\varepsilon\iota(r))]}$$

ix. $Y = \dfrac{-\beta - \frac{\alpha}{2}\frac{\sinh(2\alpha\varepsilon\iota(r))}{1+\sinh^2(\varepsilon\iota(r))} - \varepsilon\iota'(r)J(kr)}{\sqrt{\Big(\eta\mu_2 + \frac{P_2}{2}\Big)(1 + \sinh^2\varepsilon\iota(r))}}$ and we assume

$$J(kr) = \frac{krJ_1'(kr) - J_1(kr)}{r}$$

x. $N = \dfrac{Sk^2J_1''(kr)}{RJ_1(kr)} + \dfrac{SkJ_1'(kr)}{RrJ_1(kr)} + \dfrac{\rho\omega^2}{R} - \dfrac{S}{Rr^2} - \dfrac{1}{4}\Big(\dfrac{2QkJ'(kr)}{RJ_1(kr)} + \dfrac{Q}{Rr}\Big)^2$

References

1. Adkins J.E., Rivlin R.S., 1955, Large elastic deformations of isotropic materials X. Reinforcement by inextensible cords, *Philosophical Transactions of the Royal Society of London. Series A, Mathematical and Physical Sciences*, **248**, 944, 201-223
2. Akbarov S.D., Kepceler T., Egilmez M.M., 2011, Torsional wave dispersion in a finitely prestrained hollow sandwich circular cylinder, *Journal of Sound and Vibration*, **330**, 18-19, 4519-4537

3. Belfield A.J., Rogers T.G., Spencer A.J.M., 1983, Stress in elastic plates reinforced by fibres lying in concentric circles, *Journal of the Mechanics and Physics of Solids*, **31**, 1, 25-54

4. Biot M.A., 1940, The influence of initial stress on elastic waves, *Journal of Applied Physics*, **11**, 8, 522-530

5. Chattopadhyay A., Gupta S., Kumari P., Sharma V.K., 2011, Propagation of torsional waves in an inhomogeneous layer over an inhomogeneous half-space, *Meccanica*, **46**, 671-680

6. Chattopadhyay A., Gupta S., Sharma V.K., Kumari P., 2009, Reflection and refraction of plane quasi-P waves at a corrugated interface between distinct triclinic elastic half spaces, *International Journal of Solids and Structures*, **46**, 17, 3241-3256

7. Dhua S., Singh A.K., Chattopadhyay A., 2015, Propagation of torsional wave in a composite layer overlying an anisotropic heterogeneous half-space with initial stress, *Journal of Vibration and Control*, **21**, 10, 1987-1998

8. Gupta S., Bhengra N., 2017a, Dispersion study of propagation of torsional surface wave in a layered structure, Journal of Mechanics, 33(3), 303-315.

9. Gupta S., Bhengra N., 2017b, Implementation of finite difference approximation on the SH-wave propagation in a multilayered magnetoelastic orthotropic composite medium, Acta Mechanica, 228(10), 3421-3444.

10. Gubbins D., 1990, *Seismology and Plate Tectonics*, Cambridge University Press, Cambridge

11. Kaur J., Tomar S.K., 2004, Reflection and refraction of SHwaves at a corrugated interface between two monoclinic elastic halfspaces, *International Journal for Numerical and Analytical Methods in Geomechanics*, **28**, 15, 1543-1575

12. Kaur J., Tomar S.K., Kaushik V.P., 2005, Reflection and refraction of SH-waves at a corrugated interface between two laterally and vertically heterogeneous viscoelastic solid half-spaces, *International Journal of Solids and Structures*, **42**, 13, 3621-3643

13. Markham M.F., 1970, Measurements of elastic constants of fibre composite by ultrasonics, *Composites*, **1**, 145-149

14. Maugin G.A., 1981, Wave motion in magnetizable deformable solids, *International Journal of Engineering Science*, **19**, 3, 321-388

15. Ozturk A., Akbarov S.D., 2009, Torsional wave propagation in a pre-stressed circular cylinder embedded in a pre-stressed elastic medium, *Applied Mathematical Modelling*, **33**, 9, 3636-3649

16. Selim M.M., 2007, Propagation of torsional surface waves in heterogeneous half-space with irregular free surface, *Applied Mathematical Sciences*, **1**, 29, 1429-1437

17. Singh M.K., Sahu S.A., 2017, Torsional wave propagation in a pre-stressed structure with corrugated and loosely bonded surfaces, *Journal of Theoretical and Applied Mechanics, Sofia*, **47**, 4, 48-74

18. Spencer A.J.M. 1972, *Deformation of Fiber-Reinforced Materials*, Oxford University Press, London

Manuscript received December 13, 2019; accepted for print March 24, 2020